Surface reconstructions of In on Si(111)

J. Kraft, M. G. Ramsey, and F. P. Netzer
Institut für Experimentalphysik, Karl-Franzens-Universität Graz, A-8010 Graz, Austria
(Received 28 May 1996; revised manuscript received 7 August 1996)

The complete phase diagram of In-induced surface reconstructions on Si(111) surfaces has been mapped by scanning tunneling microscopy (STM) and spectroscopy (STS). The spectroscopy results illustrate the transition from low-coverage semiconducting reconstructions via semimetallic phases to the metallic surfaces at monolayer coverages. Electronic effects in the STM imaging process preclude a straightforward interpretation of the STM data in terms of structure models for the surfaces at intermediate coverages, but for the higher-coverage metallic phases a topographic STM analysis is possible and detailed structure models are presented. The In-Si(111) monolayer surfaces are interpreted in terms of regular adlayer structures above the first Si double layer, but discommensurate phases are observed in the presence of an external stress field, introduced by an external perturbation. [S0163-1829(97)01908-5]

I. INTRODUCTION

The evolution of metal-induced semiconductor surface structures in the transition from semiconducting to metallic overlayers with increasing adatom coverage is of prime importance for the well known, but still poorly understood Schottky barrier problem: the Schottky barrier of a given metal-semiconductor system reaches commonly its final macroscopic value at coverages, at which the interface acquires metallic properties.[1] Since the dependence of the Schottky barrier height on the interfacial geometry has been demonstrated,[2] the adsorbate-induced surface reconstructions in the monolayer regime, where the metallic character of the overlayer is normally established, determine the electrical properties of a metal-semiconductor junction. The In-Si(111) system provides a convenient arena for the study of structural and energetic phenomena of coverage-driven surface reconstructions, because the In-Si interface is nonreactive,[3] but with sufficient adatom-substrate coupling strength to support a variety of ordered surface structures from low to high In adatom coverages. Since the pioneering low-energy-electron-diffraction (LEED) work of Lander and Morrison[4] where eight two-dimensional In derived phases have been reported, a number of studies have addressed the surface phase diagram of In on Si(111).[3,5–9] Despite this wide-spread interest many problems remain unresolved. Apart from the $(\sqrt{3}\times\sqrt{3})R30°$ structure at low coverage[10] and the $(\sqrt{7}\times\sqrt{3})$ structure at monolayer In coverage[11] the surface reconstructions at intermediate coverages remain poorly understood, and even their respective adatom coverage ranges are uncertain. It is therefore appropriate to revisit this prototypical metal-semiconductor system, which allows us to investigate step by step in a unique way the transition from semiconducting surface reconstructions via semimetallic phases to metallic overlayer surfaces.

We present in this paper the results of a comprehensive study of the surface reconstructions of In on Si(111) from low adatom coverages up to the 1–2 ML regime as obtained by scanning tunneling microscopy (STM) and spectroscopy (STS). We report an updated surface phase diagram, which confirms and clarifies previously reported structures, but also adds new surface phases, which have not been observed hitherto. As a result of electronic effects in the STM process images of semiconducting and semimetallic surface reconstructions at intermediate In coverages cannot be interpreted unambiguously, but for the higher-coverage metallic phases a topographic STM interpretation and therefore detailed structure analyses are possible. In the following, we will present first the phase diagram of the In-Si(111) interface, and then guide the reader through the sequence of structures as seen ''through the eye of the STM.''

II. EXPERIMENT

The experiments have been carried out in a custom-designed three-chamber ultra-high-vacuum (UHV) system containing LEED, Auger electron spectroscopy (AES), and STM (micro-STM, Omicron) facilities. The sample surfaces were prepared in the preparation chamber and were then transferred via a magnetically coupled transfer system from the preparation chamber into the spectrometer chamber, where LEED/AES inspection was performed; the samples were then moved to the STM stage. The base pressure in the UHV system was typically $<1\times10^{-10}$ mbar. Sample heating by electron bombardment from the back side was possible in both preparation and spectrometer chambers, and sample temperatures were measured by an infrared pyrometer and by a thermocouple, the latter in separate calibration experiments. The STM tips used were fabricated by electrochemical etching from a 0.25–0.3 mm W wire and cleaned *in situ* by electron-beam heating in a separate tip heating stage and by field evaporation.

To obtain information on the local density of states (DOS) at the surfaces constant-separation I-U curves were measured simultaneously with the STM topographs via the current-imaging tunneling spectroscopy method.[12] The STS data were averaged over many unit cells and are presented in I-U, dI/dU vs U, or in the logarithmic derivative $d\ln I/d\ln U$ vs U form. The independence of STS features on the tip-sample distance was checked by recording spectra at various z positions of the tip, and in many cases the curves shown present averages over different tip-sample distances.

 © 1997 The American Physical Society

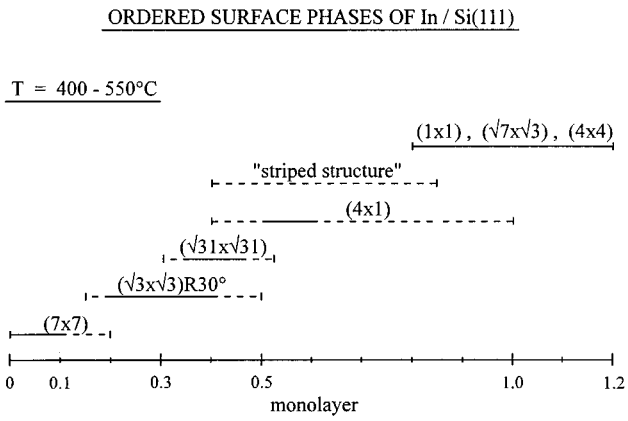

FIG. 1. Surface phase diagram of In on Si(111) for temperatures of 400–550 °C. Structures observed in STM images.

Previous studies have demonstrated a good correspondence between peaks in the logarithmic derivative and in the surface density of states,[13–15] whereas the raw I-U data reflect in the most direct way the existence of a surface-state band gap, and thus the semiconducting or metallic characteristics of a surface.

Clean, well-ordered Si(111)7×7 substrate surfaces were prepared by flashing the samples to ~1200 °C in a vacuum $<2\times10^{-9}$ mbar during the flash, and surface order and cleanliness were checked by LEED, AES, and STM. Indium was evaporated in the preparation chamber from a boron nitride crucible onto the heated Si(111)7×7 surfaces, and the evaporation rate was determined by a quartz film thickness monitor. Typically, 5 Å of In [corresponding nominally to 2.5 ML, as referred to the atomic density of the unreconstructed Si(111)1×1 substrate surface] were deposited at 400 °C, yielding the surface structures of the monolayer regime. The lower-coverage structures were generated by heating the In monolayer surfaces stepwise from 400 °C up to 550 °C. At the latter temperature the ordered structure with the lowest coverage, the $(\sqrt{3}\times\sqrt{3})$ surface, was obtained. This procedure yielded better results in terms of well-ordered surface structures than depositing the appropriate amounts of In for each structure directly onto the heated Si(111) surface. It also allowed us to establish the correct sequence of structures corresponding to decreasing surface coverages, as shown in the phase diagram in the next section.

III. RESULTS AND DISCUSSION

A. The In-Si(111) surface phase diagram

Figure 1 gives a schematic picture of the sequence of ordered surface structures of In on Si(111) with increasing In coverage, corresponding to a surface phase diagram for temperatures of ~400–550 °C. The major features of this phase diagram agree with those reported in the literature,[5–9] however the various structures around the monolayer coverage have not been explored and assigned correctly in the past, and the so-called ''striped'' structure has not been explicitly reported. It is notable that the coverage ranges of the structures in this phase diagram are somewhat uncertain as visualized by the dashed lines, and that several structures, in particular, those at intermediate coverages, overlap thereby indicating coexistence at the surface. The bar designating the (4×1) structure extends over a large coverage range (from ~0.5–1 ML), and this is due to the two competing models with different In coverages, which have been proposed in the literature.[16,17] The results of this study, however, favor somewhat the model of Stevens, Worthington, and Tsong[17] with the corresponding lower coverage of 0.5 ML, as discussed further below. It is useful, for the purpose of presentation, to divide the In-Si phase diagram into three coverage regimes: (i) the low-coverage regime with the $(\sqrt{3}\times\sqrt{3})R30°$ and the $(\sqrt{31}\times\sqrt{31})$ structures; (ii) the intermediate-coverage regime with the (4×1) and the ''striped'' structures; and (iii) the high-coverage regime up to 1–2 ML, with the (1×1), the $(\sqrt{7}\times\sqrt{3})$, and the (4×4) structures. The formation of a second-layer phase of In in form of two-dimensional In islands, which can only be observed under particular conditions, namely, in the presence of surface oxygen, will also be discussed here.

B. The low-coverage reconstructions: the $(\sqrt{3}\times\sqrt{3})R30°$ and the $(\sqrt{31}\times\sqrt{31})R9°$ structure

The $(\sqrt{3}\times\sqrt{3})R30°$ structure (hereafter referred to as $\sqrt{3}$) has been investigated previously both experimentally and theoretically.[18–23] There is general agreement that the In adatoms, at 0.3-ML coverage, occupy the threefold hollow positions above a second-layer Si atom, the so-called T_4 sites. However, the details of the T_4 geometry are still under discussion. Finney *et al.*[21] on the basis of surface x-ray-diffraction experiments concluded substantial substrate relaxation in agreement with the theoretical predictions of Northrup,[18] but Woicik *et al.*[22] derived from their back reflection x-ray standing wave and surface extended x-ray-absorption fine-structure measurements that the T_4 geometry of the In/Si(111)-$\sqrt{3}$ interface is not relaxed. Very recently, Hanada, Daimon, and Ino[23] investigated the $\sqrt{3}$ structure by reflection high-energy electron diffraction and reported substantial rumpling in the second and third layers of the substrate from a rocking curve analysis, thus supporting again the view of a relaxed substrate.

Figure 2 shows constant-current empty (a) and filled state (b) STM images of the $\sqrt{3}$-In structure. While a STM of the $\sqrt{3}$-In structure has been reported previously,[20] we wish to draw the attention here to an interesting observation concerning the defects in the $\sqrt{3}$ overlayer. The defects appear as dark holes at both sample bias polarities and they are associated, following Hamers and Demuth,[24] with vacancy defects V. The two images in Fig. 2 have been taken from the same surface region as recognized from the characteristic defect pattern. Whereas the vacancy defects appear dark in both empty and filled state images, we note that the atoms surrounding the vacancy appear also darker for the negative sample polarity (b). The line scans across the defects confirm that the In adatoms surrounding the vacancy are of the same apparent height as adatoms further away from the defect at positive sample bias [line scan Fig. 2(a)], but that they appear depressed for negative sample bias [Fig. 2(b)]. Obviously, the electronic structure of In atoms in the vicinity of the vacancy is influenced, and this is most pronounced for the *filled* electronic states, i.e., the filled DOS is decreased. This effect has not been observed for the case of the substi-

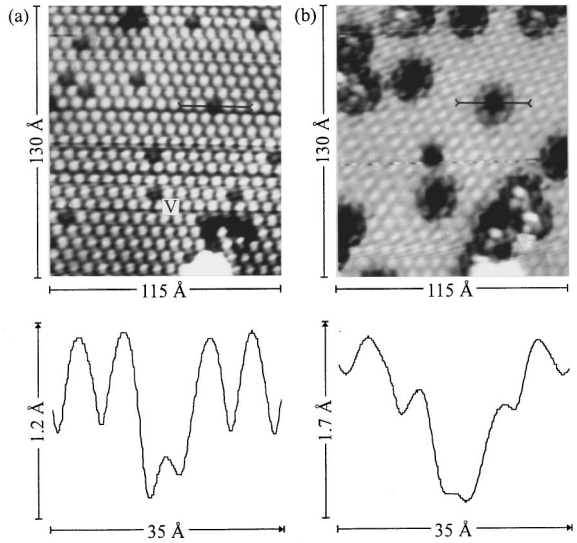

FIG. 2. Constant current topographic STM images of the ($\sqrt{3}\times\sqrt{3}$)-In structure recorded with positive (empty states imaged) (a) and negative (filled states imaged) sample bias (b) (a: +1.6 V, 0.9 nA; b: −1.6 V, 0.9 nA). The line scans below the STM pictures were taken along the respective dark lines indicated on the photographs.

tutional Si defects.[24] The decrease of the local DOS of adatoms near a vacancy defect is interesting, and may be conceptionally understood in terms of the leaking out of electronic wave functions into the vacancy hole, much in the same way as the DOS is decreased for atoms at step edges by the well-known Smoluchowski effect.[25]

With increasing In coverage of the surface the ($\sqrt{31}\times\sqrt{31}$)$R9°$ (in short $\sqrt{31}$) structure is observed in coexistence with the $\sqrt{3}$ structure. Figures 3(a) and 3(b) show high-resolution empty and filled state STM images of the $\sqrt{31}$ structure, respectively. In the empty state image (a) the structure appears ''atomically resolved,'' in that well-resolved maxima with atomic dimensions in a regular $\sqrt{31}$ array are clearly observable. The diamond-shaped $\sqrt{31}$ unit cell contains two inequivalent triangular subunits, with six and ten maxima of different contrast, and in the deep corner holes of the unit-cell lower-lying maxima are also visible. However, the filled state image [Fig. 3(b)] displays a very different appearance with lack of ''atomic resolution,'' and it is doubtful, whether a simple geometric interpretation of the STM images is possible.

Park, Nogami, and Quate[8] have based a simple adlayer model of the $\sqrt{31}$ reconstruction on a geometric interpretation of STM images such as seen in Fig. 3(a), and have derived an In coverage of 0.52 ML for this structure. Gai *et al.*[26] have recently proposed a more sophisticated, substitutional model for the related $\sqrt{31}$ structure of In on Ge(111), in which the In adatoms replace all the Ge atoms of the top layer of the first Ge double layer and also some second-layer Ge atoms (those by the deeper-lying In atoms at the corner holes). However, again a purely topographic interpretation of the STM images is at the root of this model, which is therefore only speculative. In view of the electronic effects in the STM images as demonstrated above we feel that the STM results alone are insufficient for a reliable interpretation of the $\sqrt{31}$ reconstruction and that additional information from other techniques is necessary. One particular problem with applying other, e.g., diffraction techniques, to the $\sqrt{31}$ structure is that we failed to produce a single phase $\sqrt{31}$-In structure on Si(111): this structure was always found in coexistence with the adjacent structures in the phase diagram, viz., the $\sqrt{3}$ or the (4×1) structure.

STS spectra of the $\sqrt{3}$ and $\sqrt{31}$ reconstructions are presented in Fig. 3(c) in I-U (lower panel) and dI/dU vs U form (upper panel). For the $\sqrt{31}$ structure STS curves of the two different triangular subunits of the unit cell are included. We note that both low-coverage In surface reconstructions

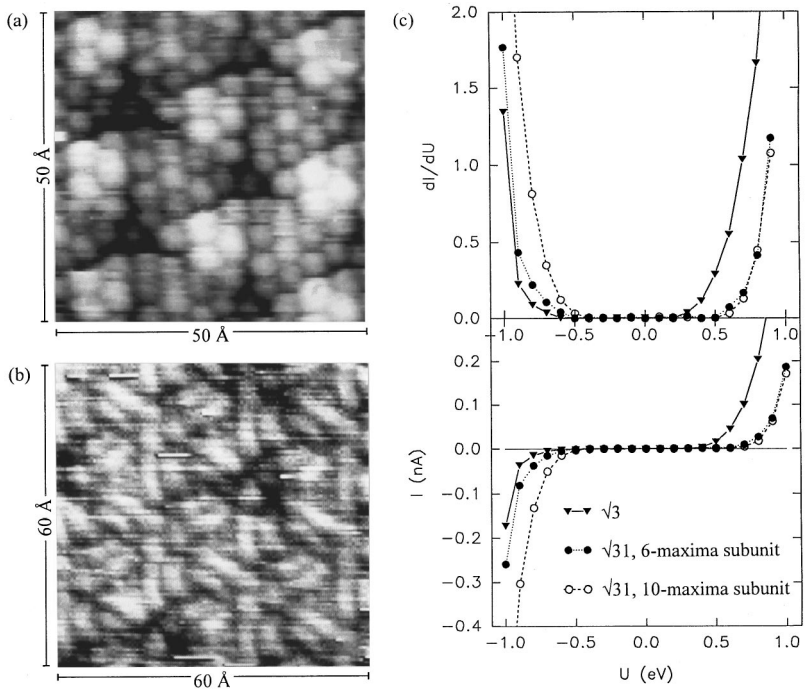

FIG. 3. Empty (a) and filled state (b) STM images of the ($\sqrt{31}\times\sqrt{31}$)-In structure (a: +1.5 V, 0.9 nA; b: −1 V, 0.9 nA). (c) Scanning tunneling spectra of the ($\sqrt{3}\times\sqrt{3}$) and the ($\sqrt{31}\times\sqrt{31}$) structures in I-U and dI/dU vs U form.

clearly display surface-state band gaps of the order of 1 eV, which is characteristic of semiconducting behavior. Specifically, the $\sqrt{3}$ surface band-gap amounts to ~0.95 eV, whereas the $\sqrt{31}$ structure shows different local surface band gaps for the two $\sqrt{31}$ subunits: the triangular subunit with six maxima in the empty state image 3(a) has a band gap of ~1.2 eV, while the one with ten maxima (with the lower contrast in the image) has ~1.3 eV. Moreover, it is noticed that the band edges of both structures are asymmetric with respect to the Fermi energy ($U=0$ eV).

C. The surface reconstructions at ''intermediate'' coverages: The (4×1) and the ''striped'' structure

On moving to higher In coverages in the surface phase diagram the (4×1) reconstruction is obtained. The STM picture of Fig. 4(a) shows the characteristic double rows of the (4×1) structure in coexistence with a region of the $\sqrt{31}$ structure. The rows are separated by 13.3 Å and oriented along the $\langle\underline{1}10\rangle$ directions; they also reveal an atomic-type zig-zag modulation of maxima along the rows as seen in the high-resolution image Fig. 4(b). The apparent average height difference between the $\sqrt{31}$ structure and the (4×1) structure in Fig. 4(a) is ~1 Å, which is clearly an electronic effect. Figure 4(a) demonstrates also the effect of the reversal of the bias polarity across the tunneling gap on the STM images of the (4×1) structure: in the middle of the image (arrow) the bias has been switched from −2 V (lower part) to +2 V (upper part). The change of the sample bias polarity results in a reversal of contrast in the (4×1) double rows: the deep furrows separating the double rows and the shallow minima inside the double rows at negative bias are replaced by bright-contrast chains at positive bias polarity. It is notable that high-resolution images of the (4×1) structure such as in Fig. 4(b) could only be obtained at a negative sample bias of −1−−2 V. The image 4(b) shows clearly the zig-zag chains of protrusions, which are separated along the rows (i.e., along the $\langle\underline{1}10\rangle$ directions) by 3.8 Å; this specifies the single substrate spacing of the (4×1) unit cell. The ''zig-zag separation'' of the maxima within the chains is more difficult to measure because of their width and the shallow minima between them, but an average separation of ~5 Å is estimated. This latter distance is of relevance for the discussion of the different structure models of the (4×1) structure.

The electronic structure of the (4×1) reconstruction is reflected in the STS spectra of Fig. 4(c). Most significantly, the I-U curve has a positive gradient around the Fermi energy ($U=0$ eV) and therefore indicates a finite DOS at E_F. The logarithmic derivative curve in Fig. 4(c) has maxima at around −0.5 and +0.4 eV, and weaker features within 0.1–0.2 eV of both sides of E_F. The prominent peak at −0.5 eV shows good correspondence with a feature in the angle-resolved photoemission spectra of Öfner *et al.*[27] at a similar energy, but the structures in the unoccupied states at around +0.4 eV and near the Fermi energy are not reflected in their inverse photoemission spectra.[27] Öfner *et al.* thus concluded that the (4×1) surface is semiconducting. More recently, Abukawa *et al.*[28] have investigated a single-domain (4×1)-In structure on a vicinal Si(111) surface by angle-resolved photoemission, and found surface states that cross the Fermi level; accordingly, they concluded that the surface

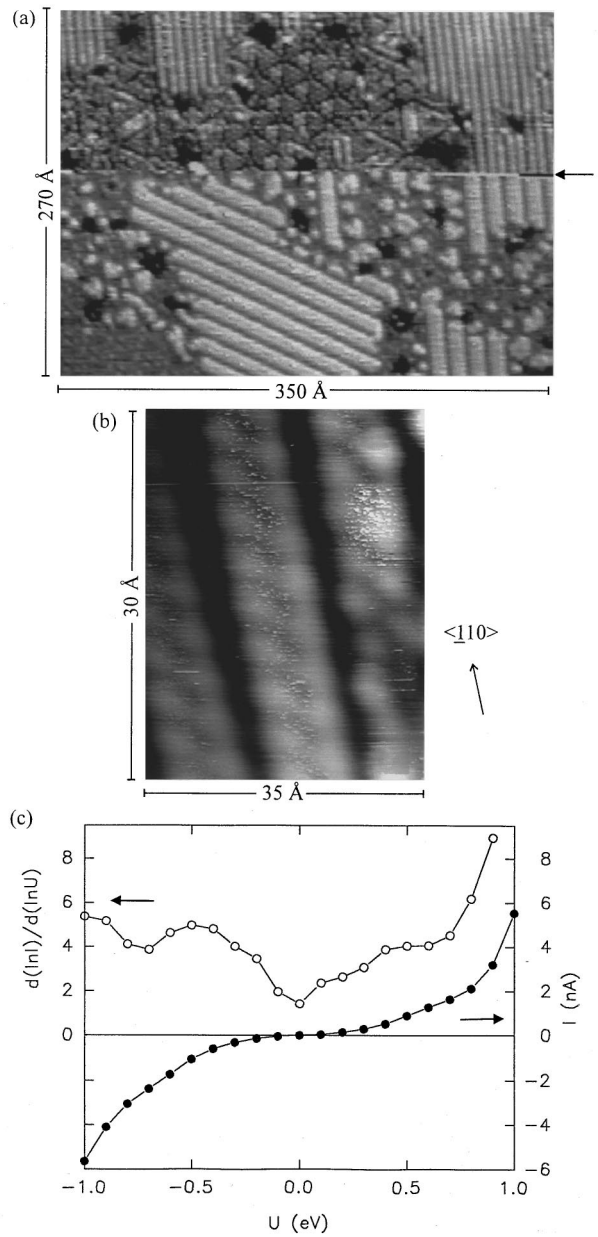

FIG. 4. (a) STM topograph of the (4×1)-In structure and coexisting regions of the ($\sqrt{31}\times\sqrt{31}$) structure. The sample bias has been switched from negative (lower part) to positive (upper part) in the middle of the image (arrow) (±2 V, 1 nA). (b) High-resolution image of the (4×1) double rows (−1.5 V, 0.5 nA). (c) STS spectra of the (4×1) surface in I-U and $d\ln I/d\ln U$ vs U form.

is metallic, in accordance with the present STS results. However, in view of the much lower DOS around E_F as compared to the In surface reconstructions at higher coverages (see below) and the electronic effects evidenced by the polarity dependence of the STM images, we prefer to characterize the (4×1) surface as semimetallic.

Two competing models of the (4×1) reconstruction have been proposed in the literature. Nakamura, Anno, and Kono[16] have suggested, on the basis of Auger electron-diffraction measurement, a structure with a coverage of 1.0 ML, in which the In adatoms occupy T_4, H_3, and bridge sites and in which the nearest-neighbor In separations, in domains of four rows along the $\langle\underline{1}10\rangle$ directions, are ~3.3 Å.

It is unclear how this model could incorporate the present high-resolution STM images. An alternative structure model has been proposed by Stevens, Worthington, and Tsong[17] to interpret impact-collision ion-scattering experiments. This model contains In adatoms in T_4 and H_3 positions, forming a zig-zag chain along the $\langle \underline{1}10 \rangle$ direction, and yields an In coverage of 0.5 ML. If a topographic interpretation of the high-resolution STM images [such as in Fig. 4(b)] is valid, the atomic distances derived from the STM agree well within the error limits with the geometry of this model. Moreover, the coverage of 0.5 ML for the (4×1) structure is in accord with the sequence of structures observed experimentally when progressing through the In-Si phase diagram.

A geometric interpretation of the high-resolution STM images of the (4×1) structure, taken at negative 1–2 V bias conditions as shown in Fig. 4(b), may not be completely without justification, however. Both Öfner *et al.*[27] and Abukawa *et al.*[28] have observed occupied surface states on the (4×1) surface in the energy region 1–1.5 eV below E_F, and the latter authors have suggested a dangling bond sp^3-type origin for these surface states. Since the corresponding orbitals are pointing towards the surface normal, the electrons tunneling out of these states in the STM process might indeed provide information on the locus of the In adatoms.

Finally, we wish to comment on a recent surface x-ray-diffraction study of the (4×1)-In structure by Finney *et al.*[29] The analysis of these data has been based on the model of Nakamura *et al.*, and an average nearest-neighbor In-In bond length of 3.07 Å in the surface unit mesh has been derived. This corresponds to an 8% bond-length contraction as compared to the In bulk, which we consider as unrealistic, particularly in view of the results obtained on the saturated In monolayer surfaces, as discussed in the next section.

In the coverage regime of the (4×1) reconstruction another structure is frequently observed as a minority phase, as shown in Fig. 5(a). Two regions of the (4×1) double rows on two terraces are readily recognized in the STM image, and they are separated by a structure on the upper terrace, which displays finer stripes. The upper left-hand-side corner of the photograph also contains a region of this structure. Two domains of the stripes are observed in Fig. 5(a), which are rotated by 30° with respect to the corresponding domain of (4×1) rows. Figure 5(b) shows another example of the coexistence of this structure, designated as ''striped,'' with the (4×1). As apparent from this image the stripes seem to consist, similar to the (4×1) chains, of a zig-zag arrangement of maxima, but the separation of the stripes is narrower than that of the (4×1) double rows.

High-resolution STM images of the ''striped'' structure are difficult to obtain, but Figs. 5(c) and 5(d) show two somewhat successful attempts. The stripes are well recognized here, but the zig-zag pattern is only just apparent; careful inspection reveals that adjacent zig-zag chains are sometimes ''in phase'' and sometimes ''out of phase,'' the antiphase domain boundaries varying arbitrarily [see arrows in Fig. 5(c)]. The chains appear to be separated by ~7.5–9.5 Å. We believe that the ''striped'' structure has also been observed by Park, Nogami, and Quate,[8] but these authors misindexed it as $(\sqrt{7}\times\sqrt{3})$. However, the structure does not really possess a periodic unit cell, and a LEED pattern particular to this structure has therefore not been detected. We have investigated several models for the ''striped'' structure based on geometric suggestions of the STM images, including a one-dimensional discommensurate phase as suggested for In on Ge(111) (Ref. 30) with statistically distributed domain widths. The models yield In coverages between 0.45–0.6 ML, however the STM resolution obtained was insufficient for further distinction.

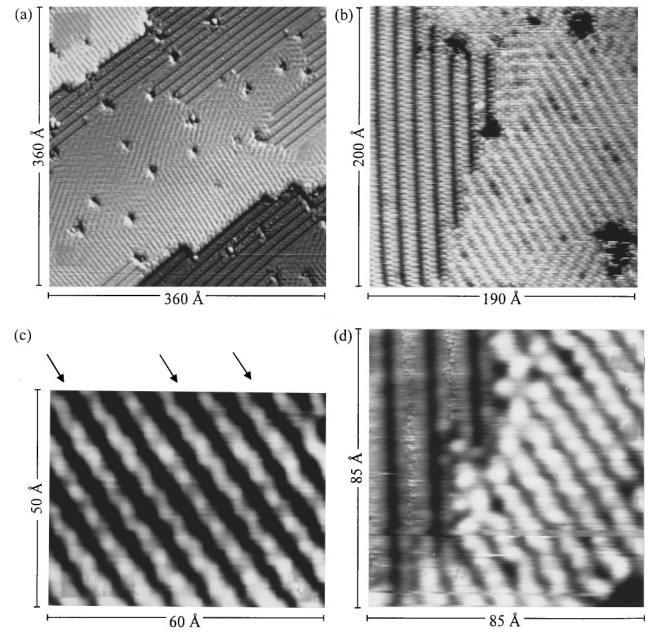

FIG. 5. STM images of the ''striped'' structure in coexistence with the (4×1) structure (a,b) (a: −2V, 2 nA; b: −0.7 V, 4 nA). (c) and (d) High-resolution STM images of the ''striped'' structure (c: +0.9 V, 2.1 nA; d: +1 V, 9.7 nA). The arrows above the image (c) denote antiphase domain boundaries.

D. The surface reconstructions around one-monolayer coverage: the $(\sqrt{7}\times\sqrt{3})$, (1×1), (4×4) structures and second-layer In islands

As the In adatom coverage approaches one monolayer the $(\sqrt{7}\times\sqrt{3})$ reconstruction (referred to in the following simply as $\sqrt{7}$) becomes the dominant surface structure. This has been detected first by LEED,[31] and has then been confirmed by STM observations.[11] Figure 6(a) shows a filled state STM image of the $\sqrt{7}$ structure, revealing maxima of atomic dimensions in a corrugated quasihexagonal array. The STM images are insensitive to the bias polarity, and for obtaining atomic-type resolution low tunnel resistances are necessary. Because of this and the metallic behavior of the In-Si surfaces at monolayer coverages in STS (see below), we associate the maxima in the high-resolution STM pictures with In adatoms, thus adopting a topographic interpretation of the STM data. In view of the quasihexagonal appearance of the structure in Fig. 6(a) this surface has been designated as $\sqrt{7}$- hex. The $\sqrt{7}$ designation is, however, not quite the correct notation, which requires a matrix description, yielding

$$\begin{vmatrix} 2 & -1 \\ 1 & 2 \end{vmatrix},$$

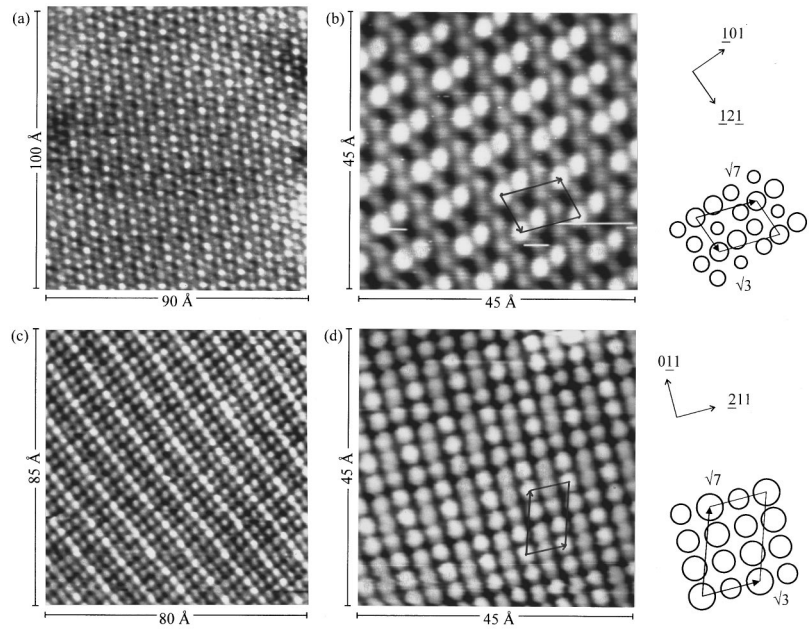

FIG. 6. STM images of the $(\sqrt{7}\times\sqrt{3})$ structures. (a) The quasihexagonal $\sqrt{7}$-hex structure (−0.012 V, 2 nA). (b) High-resolution image of the $\sqrt{7}$-hex (−0.2 V, 1 nA). (c) The quasirectangular $\sqrt{7}$-rect structure (−0.14 V, 4.1 nA). (d) High-resolution image of the $\sqrt{7}$-rect (−0.02 V, 1.4 nA). The schematic drawings illustrate the adatom contents of the two different $(\sqrt{7}\times\sqrt{3})$ unit cells, with the size of the circles representing approximately the contrast in the corresponding STM images.

(Ref. 11); because of the dimensions of the unit-cell vectors we have adopted the simplified $(\sqrt{7}\times\sqrt{3})$ notation. The high-resolution image of Fig. 6(b) reveals that the surface structure consists of a periodic arrangement of tetramers along the $\langle\underline{1}10\rangle$ direction, containing two pronounced maxima flanked by two lower-contrast atoms, which are separated periodically by a lower-contrast atom. The tetramers are displaced between adjacent rows, thus specifying the observed $(\sqrt{7}\times\sqrt{3})$ periodicity (see unit cell indicated on the photograph). The schematic drawing of the unit cell to the right-hand side of the photograph allows one to derive the In surface coverage, which is exactly 1.0 ML.

On surfaces, where the In-$\sqrt{7}$-hex structure was observed, a second reconstruction was always detected in coexistence, which displays the *same* $(\sqrt{7}\times\sqrt{3})$ *periodicity of the unit cells*, but a *very different local symmetry* and *atomic arrangement*. This is shown in Figs. 6(c) and 6(d). A quasirectangular mesh of adatoms is recognized here, and the $(\sqrt{7}\times\sqrt{3})$ unit-cell periodicity is introduced by a periodic corrugation of the adlayer; this structure has therefore been designated as $\sqrt{7}$-rect. The schematic drawing of the unit cell in Fig. 6(d) indicates that the $\sqrt{7}$-rect unit cell contains one additional adatom as compared to the $\sqrt{7}$-hex, thus giving a local coverage of 1.2 ML.

A pertinent question in this context is whether the $\sqrt{7}$-In structures are indeed true monolayer structures or whether they involve a second In layer. This question has been addressed in a previous publication,[11] where the apparent height differences in STM between coexisting (4×1) and $\sqrt{7}$ structures have been investigated. The answer to this problem is not trivial, because electronic effects tend to disguise the geometric information. However, several experimental indications provide indirect evidence that the $\sqrt{7}$ surfaces contain a *single layer* of In adatoms.[11]

The two In-$\sqrt{7}$ surface reconstructions on Si(111) have been investigated previously in detail in our laboratory, and structure models have been proposed.[11] In brief, the $\sqrt{7}$-hex has been interpreted as derived from a highly stressed pseudomorphic (1×1) In-Si structure [mismatch between In and Si(111) lattices ~15%], in which the surface strain is relieved by a periodic linear contraction (the tetramer formation) and a concomitant introduction of a single-atom misfit dislocation.[32] The coexisting $\sqrt{7}$-rect structure has been associated with the coincidence lattice of a close-packed In(001)-type overlayer on an unreconstructed Si(111)1×1 surface. The latter structure reflects the tendency to maximize the surface coverage in the first layer, and thus reveals a new driving mechanism for adsorbate-induced surface reconstructions, namely, to optimize the adsorption energy.[32] The fact that the two $\sqrt{7}$ surface structures are *always* observed in coexistence on the same surface indicates that the total energy of the two structures is balanced.

In the vicinity of surface defects or step edges an In-derived (1×1) surface structure has been observed in addition to the $\sqrt{7}$ reconstructions on the saturated In monolayer surfaces. Figure 7(a) shows a step edge in perspective view at the lower right-hand side, which is decorated by a hexagonal (1×1) arrangement with 3.8-Å nearest-neighbor distances, while the $\sqrt{7}$-rect structure is recognized on the terrace further away from the step edge. In Fig. 7(b) an area with large defect regions of the overlayer has been imaged, which shows again the decoration of the defect boundaries by the (1×1) structure. The (1×1) structure exhibits metallic properties, and this supports its assignment as an In-derived adatom structure. As mentioned above the (1×1) In-Si configuration is highly strained, and this may be the reason why the (1×1) structure is only observed near surface defects, where the surface stress can be released. The experimental detection of the In-Si (1×1) structure at defect boundaries on the In monolayer surfaces is an important observation to substantiate the strain-relief model of the $\sqrt{7}$-hex reconstruction.[32]

The delicate energetic balance of the $\sqrt{7}$ In monolayer surfaces is illustrated by the application of an external stress field, which destabilizes these structures and introduces new structural phenomena. The external perturbation may be ap-

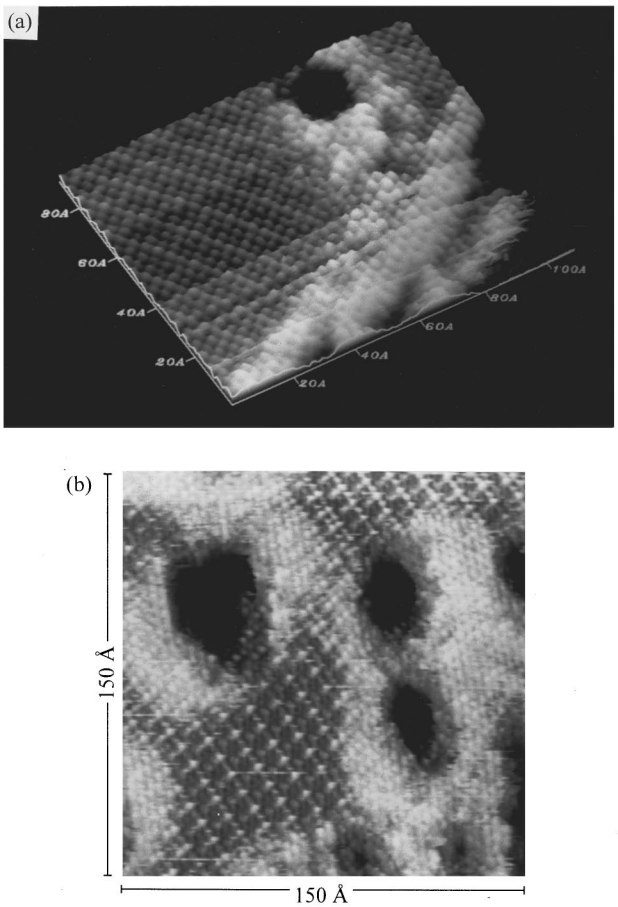

FIG. 7. (a) STM image of a terrace with the $\sqrt{7}$-rect structure and of a step edge (running across in the lower right-hand-side corner), in a perspective view (-0.14 V, 4.1 nA). Note that the step edge is decorated with a hexagonal (1×1) structure. (b) STM image of the In monolayer surface with overlayer defect regions, showing the decoration of defect areas with the (1×1) structure and areas of the $\sqrt{7}$-hex structure (-0.006 V, 7 nA).

plied by the electric field of the scanning STM tip, when repeatedly scanned over the same surface region, or by the stress field resulting from the nonlocal chemical effects of reactive adsorbates such as oxygen[33] or phosphorus.[34] The STM pictures of Figs. 8(a) and 8(b) show the evolution of bright-contrast maxima on the $\sqrt{7}$ surfaces after repeated scanning of the tip over the same area; the appearing maxima are arranged in an approximate (4×4) array. The high-resolution STM images of Figs. 8(c)–8(e), taken at various tunneling conditions, disclose interesting details of this ''(4×4)'' structure. Figure 8(c) shows very clearly a (4×4) array of circular blobs, with diameters $\sim$10 Å, but gives no details of their internal structure, whereas the images (d) and (e) reveal that the structure consists of (1×1) domains of variable sizes and shape, which are separated by domain walls of lower contrast. The surface is metallic as evidenced by STS and thus also an In adatom-derived structure, but no LEED pattern corresponding to the (4×4) structure has been observed. The most natural interpretation of this structure, which is induced by external perturbations, is therefore in terms of a discommensurate phase with small domains of a (1×1) adatom arrangement, separated by strain-relieving domain walls (lower contrast in the STM images). This domain-structure model is supported by the observation that occasionally the long-range periodicity is noninteger, e.g., (5.5×5.5) or the like.

The study of the formation of a second layer of In atoms on top of the ordered In-Si monolayer surfaces is of interest for the growth mechanism of In films on Si surfaces, and also of general relevance for Stranski-Krastanov-type film growth models. It has been reported previously that the deposition of In onto the $\sqrt{7}$-In monolayer surfaces at both room and elevated temperatures results in a peculiar growth pattern:[35] the In atoms do not wet the $\sqrt{7}$ surface, the mobility of In atoms on the smooth In monolayer surfaces (note that the maximal corrugation on the $\sqrt{7}$ surfaces is $\sim$0.25 Å) is very high, and even large amounts of evaporated In (several hundred Å) agglomerate in only a few droplets with ''macroscopic'' (i.e., μm) dimensions. However, in the presence of surface oxygen the mobility of In atoms on the $\sqrt{7}$ surfaces is drastically reduced,[36] and second-layer In atoms have been observed to condense into two-dimensional pure In island structures. Figure 9(a) shows a $\sqrt{7}$ surface, exposed to 700 L [1 Langmuir (L)$=1\times10^{-6}$ Torr sec] O_2 and subsequently dosed with 0.2 ML of In at room temperature. Indium island structures (one is marked A) are recognized in the picture, in addition to regions containing the unperturbed $\sqrt{7}$ structure, the (4×4) structure, and a $(\sqrt{3}\times\sqrt{3})$ structure which has been ascribed to adsorbed oxygen.[33] The line scan across the island boundary [Fig. 9(b)] specifies a step height of $\sim$2.7 Å, in accord with a single layer of In atoms. The most interesting feature of this two-dimensional In island is the fact that it is grown in epitaxial order: atomic resolution STM images have been obtained on the island surface, as shown in Fig. 9(c). A hexagonal arrangement of atoms is seen in this picture, with nearest-neighbor distances of 3.8 Å, thus with the dimensions of the Si(111)1×1 lattice. The 2D island is therefore grown in a pseudomorphic fashion, and the underlying In monolayer has presumably been rearranged into a (1×1) structure, thus mediating the Si substrate geometry. The formation of a second layer of In on Si(111) in a pseudomorphic geometry has been inferred by Finney *et al.*[37] from x-ray reflectivity and Auger electron spectroscopy measurements. Their value derived for the height of the second In layer of 2.6 ± 0.1 Å agrees well with the present STM value. It is unclear, however, why Finney *et al.* seem to have observed second-layer formation at a Si substrate temperature of $\sim$400 °C, whereas our studies have shown that the pristine $\sqrt{7}$ monolayer surfaces do not allow the formation of a second In layer due to the high In adatom mobility on this surface.[35]

The STS spectra of the high-coverage In-Si surfaces are summarized in Fig. 10. The I-U plots (panel a) indicate clearly the metallic character of the surfaces and thus support the employed topographic interpretation of the STM images; the In adatom nature of the reconstructions and the In character of the 2D island structures are also confirmed by these data. The differentiated STS curves (panel b) of the $\sqrt{7}$ and the (4×4) surfaces reveal a similar course, with common features at around -0.3–0.4 eV and $+0.3$–0.4 eV. This points towards a general similarity of these reconstructions (e.g., the same surface coverage). The 2nd layer In islands also show a similar STS structure to the monolayer surfaces

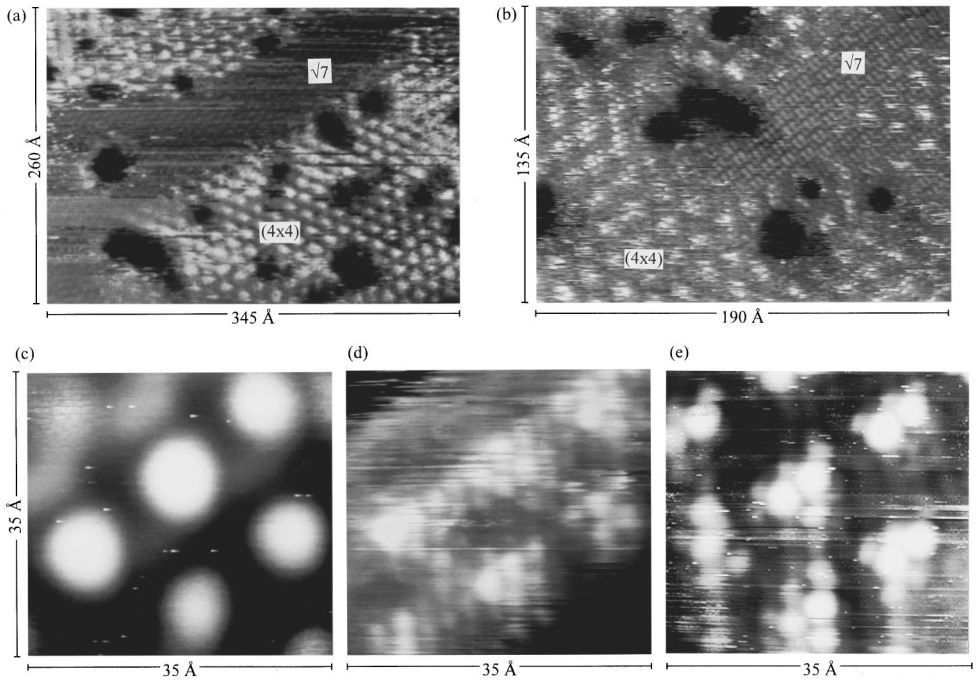

FIG. 8. STM images of the ''(4×4)'' structure, which forms in the presence of an external stress field, introduced by an external perturbation. (a) and (b) STM images showing the emerging maxima in a (4×4) array from the original ($\sqrt{7}\times\sqrt{3}$) structure (a: −0.026 V, 1.9 nA); (b: −0.017 V, 1.9 nA). (c)–(e) High-resolution images of the (4×4) structure at different bias values (c: −2 V, 0.1 nA; d: −0.14 V, 3.3 nA; e: −0.09 V, 5.5 nA).

indicating a generally similar electronic behavior of the high-coverage In overlayer surfaces, with a tendency to converge towards the In bulk electronic structure.

IV. CONCLUSIONS

We have investigated in this paper the ordered surface reconstructions of In on Si(111), from the low-coverage regime to the In monolayer phases, and thus specified the complete In-Si(111) phase diagram using scanning tunneling microscopy and spectroscopy. At low In coverages, the resulting surfaces are semiconducting whereas the monolayer surfaces are metallic as manifested by the STS spectra, but the transition region at intermediate coverages is described best in terms of semimetallic phases.

It is of interest at this point to compare the In-Si surface phase diagram with those of the related Al- and Ga-Si(111) systems. At low coverages, i.e., around 1/3 ML, all three metals form ($\sqrt{3}\times\sqrt{3}$) structures, with the adatoms in the threefold hollow T_4 positions,[10] but after this common starting ground the phase diagrams diversify. For Al/Si(111) a ($\sqrt{7}\times\sqrt{7}$) structure at $\Theta_{Al}=\frac{3}{7}$ (Ref. 38) is followed by the so-called γ phase at around 1-ML coverage[39] [designated also as (7×7) (Ref. 38) or (9×9) (Ref. 40)]; for Ga/Si(111) a (6.3×6.3) and other complex structures such as a (11×11) have been reported for $\Theta_{Ga}>0.6$.[41–43] The higher-coverage Al and Ga surface reconstructions have been interpreted in terms of substitutional adsorption sites (i.e., adatoms substituting for the Si atoms of the top layer of the first Si double layer) and have been associated with discommensurate surface phases containing domain-wall superstructures. This is different from the In/Si(111) system, where the monolayer saturation surfaces, the ($\sqrt{7}\times\sqrt{3}$) structures, may be interpreted as ''regular'' adlayer structures, with the adsorbed In atoms located on the top of the first Si double layer. Discommensurate phases have only been observed in the presence of an additional stress field introduced by external perturbations.

Following Meade and Vanderbilt[44] the principal sources of surface stress on chemisorbed semiconductor surfaces are the atomic size of the adsorbate with the associated adsorbate-substrate mismatch and the chemical bonding topology. In view of the electronic similarity of the three group-III elements the hybridization of the adatoms is expected to be similar, leaving the adatom size as a distinguish-

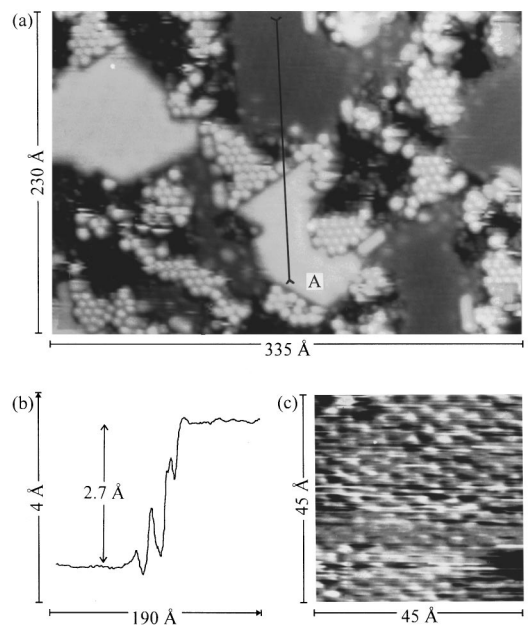

FIG. 9. (a) STM image of a ($\sqrt{7}\times\sqrt{3}$)-In surface exposed to 700 L O_2 and subsequently dosed with additional 0.2 ML of In at room temperature. The bright-contrast ($\sqrt{3}\times\sqrt{3}$) structure is ascribed to adsorbed oxygen and the dark areas are the original $\sqrt{7}$-In structure. A second-layer In island is marked by (A) (−2.1 V, 0.7 nA). (b) Line scan across the island boundary along the dark line as indicated in the photograph (a). (c) High-resolution STM image of the top surface of the In island A (−0.2 V, 2.5 nA).

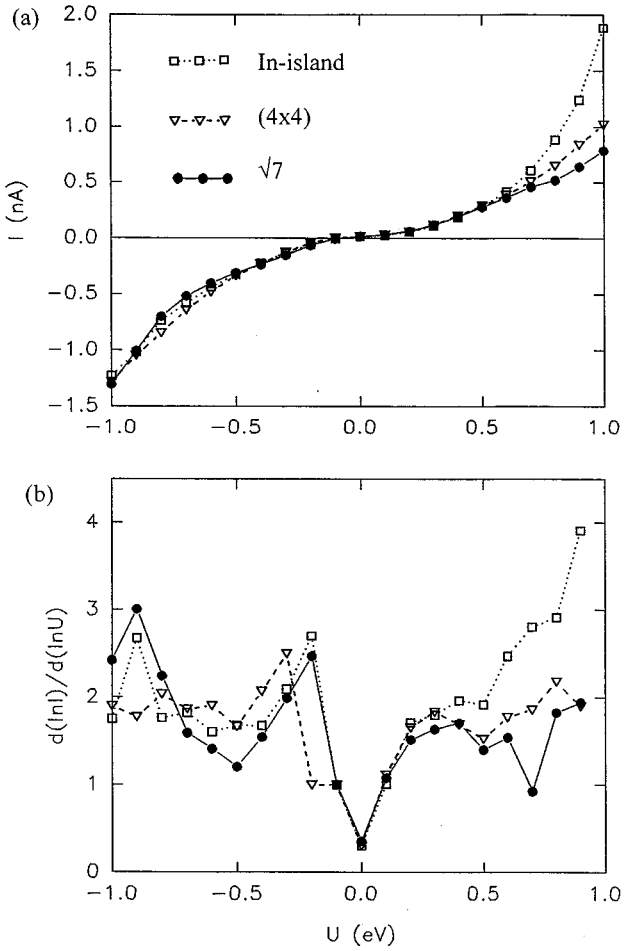

FIG. 10. STS spectra of the $\sqrt{7}$ and (4×4) surfaces and from a second-layer In island in I-U (a) and $d \ln I/d \ln U$ vs U form (b).

ing effect. The adsorbate-Si bonding involving sp^2 hybridization provides the driving force for the substitutional adatom geometries of the Al and Ga adlayers, which are inward relaxed to achieve an almost planar Al(Ga)-Si geometry in the (1×1) substitutional layer. As a result of the adsorbate-Si bonding the chemisorbed surfaces are under tensile stress, which leads to the introduction of discommensurations[45] as mentioned above. Figure 11, which has been adapted from Meade and Vanderbilt,[44] presents a plot of the ideal bond length between Si and chemisorbed group-III species predicted from covalent radii (circles) and of the bond lengths calculated on relaxed substitutional 1×1

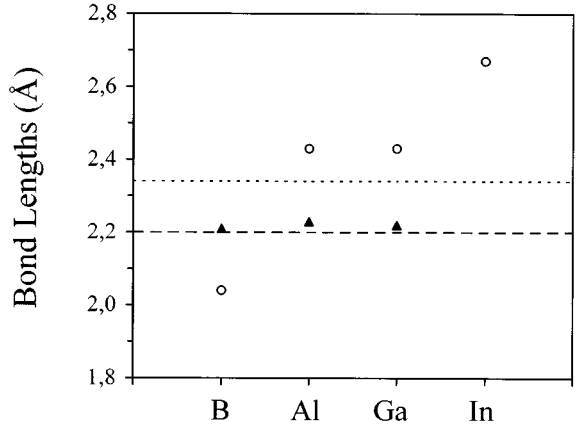

FIG. 11. Ideal bond lengths between Si and chemisorbed species predicted from covalent radii (circles) and calculated on relaxed (1×1) Si(111) surfaces (triangles). Surfaces in which relaxed bond lengths are less (greater) than ideal bond lengths are under tension (compression). Dashed line is minimum bond length allowed on (1×1) surfaces, dotted line represents ideal Si-Si bond length. Adapted from Ref. 44.

Si(111) surfaces (triangles). We have added to this plot of Meade and Vanderbilt the ideal bond length (from covalent radii) for In-Si, for which the relaxed bond length has not been calculated. However, it is apparent from the diagram that the size of the In atom is clearly unfavorable for a substitutional (1×1) geometry (the in-plane geometry is indicated in Fig. 11 by the dashed line). The size of the In atom provides therefore a simplistic argument to explain why a *regular adlayer geometry on top* of the first Si double layer is encountered for In-Si(111), with the associated structural phenomena discussed in this paper. At high coverages of In on Si(111) complex structures involving some In-In distances close to those of elemental In metal emerge, but the energetic balance of bonding and size effects appears to be delicate as reflected by the coexistence of the two different ($\sqrt{7}\times\sqrt{3}$) structures and by their destabilization in the presence of external stress.

ACKNOWLEDGMENTS

This work has been supported by the Austrian Science Foundation. We are grateful to Professor J. A. D. Matthew, University of York, England, for discussions and a critical reading of the manuscript.

[1] For a compilation of relevant references, see *Electronic Structure of Metal-Semiconductor Contacts*, edited by W. Mönch, Perspectives in Condensed Matter Physics Vol. 4 (Kluwer, Dordrecht, 1990).

[2] D. R. Heslinga, H. H. Weitering, D. P. Van der Werf, T. M. Klapwijk, and T. Hibma, Phys. Rev. Lett. **64**, 1589 (1990).

[3] H. Öfner, S. L. Surnev, Y. Shapira, and F. P. Netzer, Phys. Rev. B **48**, 10 940 (1993).

[4] J. J. Lander and J. Morrison, J. Appl. Phys. **36**, 1706 (1965).

[5] M. Kawaji, S. Baba, and A. Kinbara, Appl. Phys. Lett. **34**, 748 (1979).

[6] S. Baba, M. Kawaji, and A. Kinbara, Surf. Sci. **85**, 29 (1979).

[7] M. K. Kelly, G. Margaritondo, J. Anderson, D. J. Frankel, and G. J. Lapeyre, J. Vac. Sci. Technol. A **4**, 1396 (1986).

[8] S. Park, J. Nogami, and C. F. Quate, J. Microsc. **152**, 727 (1988).

[9] S. Hasegawa and S. Ino, Int. J. Mod. Phys. B **7**, 3817 (1993).

[10] J. Nogami, Surf. Rev. Lett. **1**, 395 (1994).

[11] J. Kraft, S. Surnev, and F. P. Netzer, Surf. Sci. **340**, 36 (1995).

[12] R. J. Hamers, R. M. Tromp, and J. E. Demuth, Phys. Rev. Lett. **56**, 1972 (1986).
[13] N. D. Lang, Phys. Rev. Lett. **58**, 45 (1987).
[14] R. M. Feenstra, J. A. Stroscio, and A. P. Fein, Surf. Sci. **181**, 295 (1987).
[15] R. J. Hamers, Ph. Avouris, and F. Bozso, Phys. Rev. Lett. **59**, 2071 (1987).
[16] N. Nakamura, K. Anno, and S. Kono, Surf. Sci. **256**, 129 (1991).
[17] J. L. Stevens, M. S. Worthington, and I. S. T. Tsong, Phys. Rev. B **47**, 1453 (1993).
[18] J. M. Nicholls, P. Martensson, G. V. Hansson, and J. E. Northrup, Phys. Rev. B **32**, 13 333 (1985).
[19] J. M. Nicholls, B. Reihl, and J. E. Northrup, Phys. Rev. B **35**, 4137 (1987).
[20] J. Nogami, S. Park, and C. F. Quate, J. Vac. Sci. Technol. B **6**, 1479 (1988).
[21] M. S. Finney, C. Norris, P. B. Howes, R. G. van Silfhout, G. F. Clark, and J. M. C. Thornton, Surf. Sci. **291**, 99 (1993).
[22] J. C. Woicik, T. Kendelewicz, A. Herrera-Gomez, K. E. Miyano, P. L. Cowan, C. E. Bouldin, P. Pianetta, and W. E. Spicer, Phys. Rev. Lett. **71**, 1204 (1993).
[23] T. Hanada, H. Daimon, and S. Ino, Phys. Rev. B **51**, 13 320 (1995).
[24] R. J. Hamers and J. E. Demuth, Phys. Rev. Lett. **60**, 2527 (1988).
[25] R. Smoluchowski, Phys. Rev. **60**, 661 (1941).
[26] Z. Gai, R. G. Zhao, Y. He, H. Ji, C. Hu, and W. S. Yang, Phys. Rev. B **53**, 1539 (1996).
[27] H. Öfner, S. L. Surnev, Y. Shapira, and F. P. Netzer, Surf. Sci. **307–309**, 315 (1994).
[28] T. Abukawa, M. Sasaki, F. Hisamatsu, T. Goto, T. Kinoshita, A. Kakizaki, and S. Kono, Surf. Sci. **325**, 33 (1995).
[29] M. S. Finney, C. Norris, P. B. Howes, M. A. James, J. E. Macdonald, A. D. Johnson, and E. Vlieg, Physica B **198**, 246 (1994).
[30] M. Böhringer and J. Zegenhagen, Surf. Sci. **327**, 248 (1995).
[31] The LEED pattern of In on Si(111) at around monolayer coverages has been indexed previously as $(1\times1)R30°$ (Refs. 3, 5, 7). However, as shown by STM and discussed in detail in Ref. 11, this LEED pattern is due to the overlapping contributions of three equivalent domains of the $\sqrt{7}$ structure, and the original designation was prompted by the visual impression of the diffraction pattern at particular electron energies.
[32] J. Kraft, M. G. Ramsey, and F. P. Netzer (unpublished).
[33] J. Kraft and F. P. Netzer, Surf. Sci. **357-358**, 740 (1996).
[34] F. P. Netzer, L. Vitali, J. Kraft, and M. G. Ramsey (unpublished).
[35] S. L. Surnev, J. Kraft, and F. P. Netzer, J. Vac. Sci. Technol. A **13**, 1389 (1995).
[36] J. Kraft, Ph.D. thesis, University of Graz, 1996.
[37] M. S. Finney, C. Norris, P. B. Howes, and E. Vlieg, Surf. Sci. **277**, 330 (1992).
[38] R. J. Hamers, Phys. Rev. B **40**, 1657 (1989).
[39] E. A. Khramtsova, A. V. Zotov, A. A. Saranin, S. V. Ryzhkov, A. B. Chub, and V. G. Lifshits, Appl. Surf. Sci. **82/83**, 576 (1994).
[40] K. Nishikata, K. Muakami, M. Yoshimura, and A. Kawazu, Surf. Sci. **269/270**, 995 (1992).
[41] M. Otsuka and T. Ichikawa, Jpn. J. Appl. Phys. **24**, 1103 (1985).
[42] D. M. Chen, J. A. Golovchenko, P. Bedrossian, and K. Mortensen, Phys. Rev. Lett. **61**, 2867 (1988).
[43] J. Zegenhagen, E. Artacho, P. E. Freeland, and J. R. Patel, Philos. Mag. B **70**, 731 (1994).
[44] R. D. Meade and D. Vanderbilt, Phys. Rev. Lett. **63**, 1404 (1989).
[45] R. F. Willis, in *Dynamical Phenomena at Surfaces, Interfaces and Superlattices*, Vol. 3 of Springer Series in Surface Sciences (Springer, Heidelberg, 1985), p. 126.